Spontaneous spatio-temporal patterns of activity in thalamic reticular nucleus

M.Bazhenov[1], I.Timofeev[2], M.Steriade[2] and T.Sejnowski[1,3]

[1]Howard Hughes Medical Institute, The Salk Institute, Computational Neurobiology Laboratory, La Jolla, CA 92037

[2]School of Medicine, Laval University, Quebec, Canada G1K 7P4

[3]Department of Biology, University of California San Diego, La Jolla, CA 92093

Abstract

Recent intracellular recordings from reticular thalamic (RE) neurons at resting and hyperpolarized membrane potentials *in vivo* suggest that the reversed inhibitory post-synaptic potentials (IPSPs) between RE cells can directly trigger a low-threshold spike. The oscillatory mechanisms underlying IPSP-triggered low-threshold spikes crowned by spike-bursts within the RE nucleus and their effect on the network behavior were investigated in models of an isolated RE network and network of RE and thalamocortical (TC) cells. In a one-dimensional RE network the external stimulation resulted in waves of excitation propagating with constant velocity 25-150 cells/sec controlled by the $GABA_A$ conductance, radius of synaptic interconnections in the network and the level of membrane potential in RE cells. In a one-dimensional network of RE and TC cells sequences of spindle oscillations were followed by localized waves propagating inside the RE network, triggering oscillations involving both RE and TC cells. This model predicts that the isolated reticular nucleus may initiate sequences of spindle oscillations in thalamocortical networks *in vivo*.

1 Introduction

Sleep spindle oscillations consist of waxing–and–waning field potentials of 7-14 Hz which last 1-3 sec and recur every 5-15 sec. These oscillations are generated in the thalamus as a result of interaction between thalamocortical (TC) and thalamic reticular (RE) cells (Steriade et al., 1985; Steriade and Llinás, 1988; Steriade et al., 1990; Krosigk et al., 1993). The waxing phase of spindle oscillations is associated with recruitment of the neurons from thalamic and reticular nuclei (Steriade et al., 1993), while the waning phase occurs as a result of Ca^{2+} up-regulation of I_h current in TC cells (Bal and McCormick, 1996). The mechanisms underlying generation of sleep spindles have been investigated in the computer models of RE–TC network (Destexhe et al., 1996; Golomb et al., 1996). An increase of I_h conductance during a spindle sequence leads to the depolarization of TC cells and the termination of spindle oscillations. The oscillations were reinitiated by spontaneous activity in some of TC cells, which were able to oscillate spontaneously at the resting membrane potential (Destexhe et al., 1996).

Extracellular unit and field potential recordings from the isolated RE nucleus (Steriade et al., 1987) as well as computational modeling of RE cells (Destexhe et al.,1994a; Golomb

et al., 1994) have shown that the deafferented reticular thalamus can itself generate spindle oscillations. These results suggest a possible role of reticular nucleus in initializing of sequences of spindle oscillations in intact RE–TC network.

The synaptic stimulation of RE cells hyperpolarized below -75 mV produces a burst of action potentials (Contreras et al., 1993). The Cl^- reversal potential in RE cells is about -71 mV which is depolarized compare to the reversal potential in TC cells (Ulrich and Huguenard, 1997). Thus, at a rest membrane potential of -78 mV (Ulrich and Huguenard, 1996) a $GABA_A$ inhibitory postsynaptic potentials (IPSP) in an RE cell will be reversed and may trigger a burst of Na^+ spikes. We investigated a model of the RE network and found that when the RE cells were hyperpolarized below the Cl^- reversal potential, propagating patterns of spike–burst activity were observed, which were able to trigger sequences of spindle oscillations in a model RE-TC network.

2 Methods

2.1 Intrinsic currents

We examined single-compartment models of TC and RE cells which included voltage- and calcium-dependent currents described by Hodgkin-Huxley kinetics:

$$C_m \frac{dV}{dt} = -g_L(V - E_L) - I^{int} - I^{syn} \tag{1}$$

where $C_m = 1\mu/cm^2$ is the membrane capacitance, g_L is the leakage conductance ($g_L = 0.01mS/cm^2$ for TC cell and $g_L = 0.05mS/cm^2$ for RE cell), E_L is the reversal potential ($E_L = -70mV$ for TC cell and $E_L = -77mV$ for RE cell), I^{int} is a sum of active intrinsic currents (I_j^{int}) and I^{syn} is a sum of synaptic currents (I_j^{syn}). The area of RE cell was $S_{RE} = 1.43 \cdot 10^{-4}cm^2$ and the area of TC cell was $S_{TC} = 2.9 \cdot 10^{-4}cm^2$.

For both RE and TC cells we considered a fast sodium current I_{Na}, a fast potassium current I_K (Traub and Miles, 1991), a low–threshold Ca^{2+} dependent current I_T (Huguenard and Prince, 1992; Huguenard and McCormick, 1992), and a potassium leak current $I_{KL} = g_{KL}(V - E_{KL})$. A hyperpolarization–activated cation current I_h (McCormick and Pape, 1990; Destexhe et al., 1996) was also included in TC cells. The expressions for voltage– and Ca^{2+}–dependent transition rates for all currents are given in (Bazhenov et al., 1998).

2.2 Synaptic currents

All synaptic currents were were calculated according to

$$I_{syn} = g_{syn}[O](V - E_{syn}), \tag{2}$$

where g_{syn} is the maximal conductivity, $[O](t)$ is the fraction of open channels, E_{syn} is the reversal potential ($E^{syn}_{AMPA} = 0$ mV for AMPA receptors, $E^{syn}_{GABA_A} = -70$ mV for $GABA_A$ receptors in RE cells and $E^{syn}_{GABA_A} = -80$ mV for $GABA_A$ receptors in TC cells (Ulrich and Huguenard, 1997), $E^{syn}_{GABA_B} = -95mV$ for $GABA_B$ receptors).

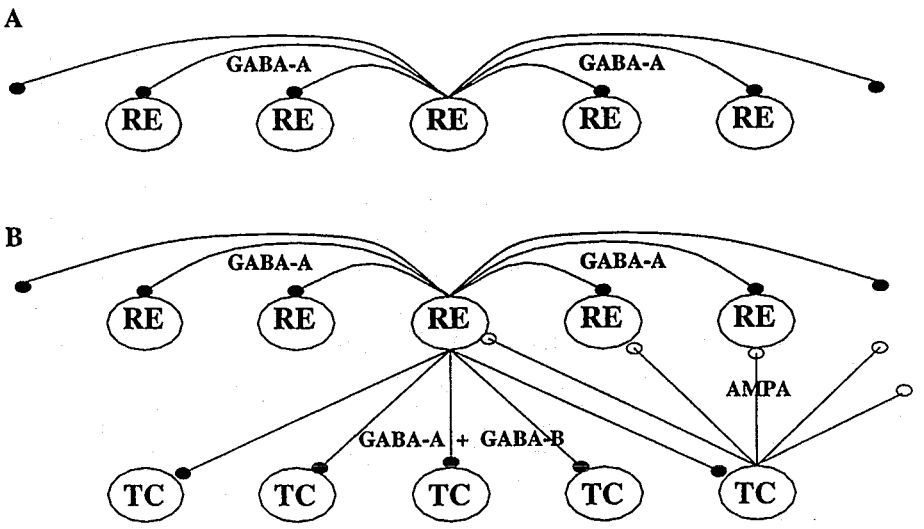

Figure 1: The pattern of synaptic interconnections in the network models. (A) Isolated RE network. (B) RE–TC network.

$GABA_A$ and AMPA synaptic currents were modeled by first-order activation schemes (see review in Destexhe et al., 1994b). $GABA_B$ receptors were modeled by a higher-order reaction scheme that took into account activation of K^+ channels by G-proteins (Dutar and Nicoll, 1988; Destexhe et al., 1994b; Destexhe et al., 1996). The equations for all synaptic currents are given in (Bazhenov et al., 1998).

2.3 Network geometry

We simulated two network models: 1) A one-dimensional chain of 100 RE cells (Fig. 1A); and 2) A one-dimensional chain of 100 RE and 100 TC cells (Fig. 1B). In the first model each RE cell was connected with 4–18 nearest neighbors with $GABA_A$ synapses. In the second model we additionally considered RE→TC ($GABA_A$ + $GABA_B$) and TC→RE (AMPA) connections. The diameters of the connection fan out were 9 cells for all types of synapses. Some of the intrinsic parameters of the neurons in the network (g_{KL}, g_h for TC cells and g_{KL} for RE cells) were initialized with some random variability (variance $\sigma \sim 10\%$) to insure the robustness of the results (Bazhenov et al., 1998).

2.4 Computational methods

All simulations described in the paper were performed using fourth-order Runge-Kutta (RK(4)) method and in some cases embedded Runge-Kutta (RK6(5)) method (Enright et al., 1995) with time step 0.04 ms. Source C++ code was compiled on a Alpha Server 2100A (5/300) using DEC C++ compiler. A simulation with 100 RE cells took 6 minutes and a network with 2×100 RE-TC cells took 28 minutes of computer time to simulate 1 sec of real time.

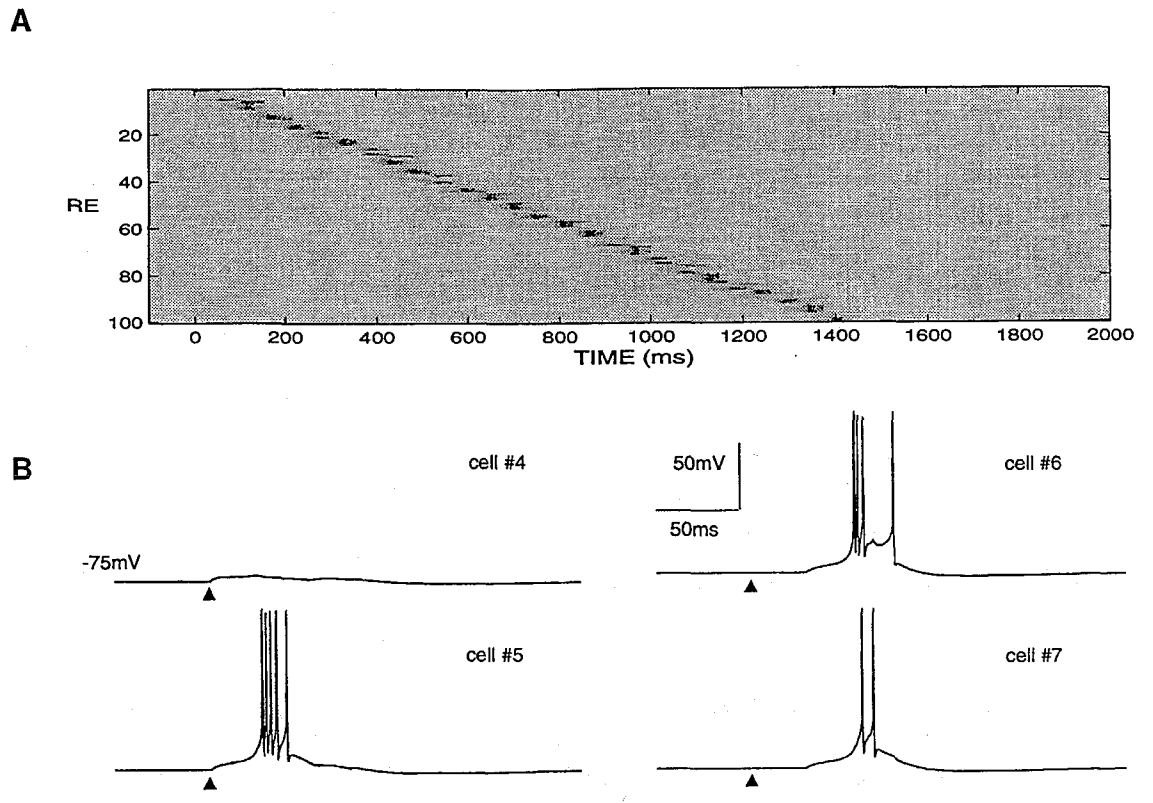

Figure 2: Localized pattern propagating through isolated RE network. (A) RE cell #1 was stimulated at $t = 0$, which triggered a localized pattern that traveled with constant velocity through RE network. (B) Four neighbor RE cells (#4 to #7) from the network are shown. Burst of spikes in one RE cell leads to a depolarizing $GABA_A$ IPSP followed by a low-threshold spike and a burst of Na^{2+} spikes in the neighboring RE cells. Temporal inactivation of the low-threshold Ca^{2+} current in RE cell after burst discharge prevents the oscillations from persisting. Triangles mark the moment of stimulation.

3 Results

3.1 Isolated RE network

Dynamical properties of the isolated RE network hyperpolarized below the Cl^- reversed potential were investigated in the network model with 100 RE cells. An external AMPA stimulus applied to the RE cell located at the boundary of the network triggered a localized pattern of spike-burst activity propagating with constant velocity through RE network (Fig. 2A). The mechanism of propagation depended on the level of membrane potential in RE cells. At the rest membrane potential of about -75 mV the low-threshold Ca^{2+} current in the RE cells was deinactivated. Burst of spikes in presynaptic RE cells led to reversed $GABA_A$ IPSPs followed by a low-threshold Ca^{2+} spike and a burst of Na^+ spikes in neighboring RE cells (Fig. 2B). The temporal inactivation of the low-threshold Ca^{2+} current in an RE cell after a burst discharge prevented oscillations from persisting in the cell. All RE cells were grouped into the clusters of 2-4 cells which fired simultaneously. These clusters were

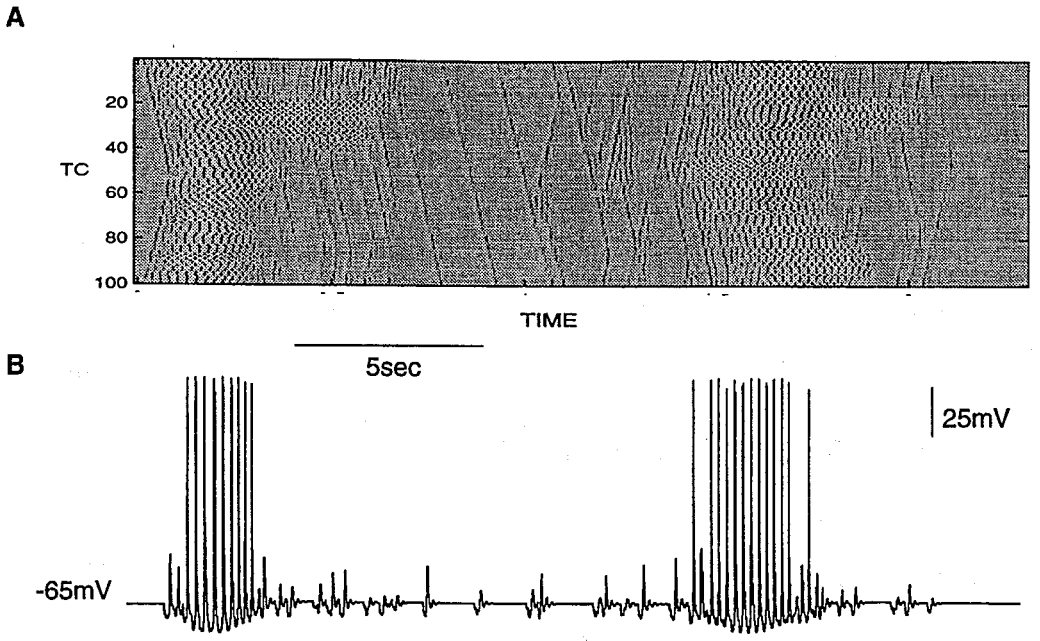

Figure 3: Role of localized patterns for initialization of spindle sequences. (A) The sequence of spindle oscillations was initialized at $t = 0$ by the local stimulation of TC cell #1 (left upper corner of the panel). After 2-4 sec the spindle sequence was terminated because of the Ca^{2+} up-regulation of I_h current. Localized pattern traveling through RE nuclei triggers a new spindle sequence at about $t = 15sec$. (B) Time evolution of membrane potential for TC cell #66.

separated by RE cells that showed reversed IPSPs with small Ca^{2+} spikes but without Na^+ spikes (see cell #4 in Fig. 2).

The waves of excitation propagated through the network with a constant velocity of 25-150 cells/sec. The speed of propagation increased with larger $GABA_A$ conductances and a larger radius of synaptic interconnections. Propagating patterns were not seen for $g_{GABA_A} < 0.04$ μS and for $g_{GABA_A} > g_{max}$, where g_{max} increased with increasing radius of synaptic interconnections. Wave activity was also absent for the networks with fan out diameter of the connections less than 6 cells.

3.2 Network of RE–TC cells

In the one–dimensional chain of RE–TC cells the external AMPA stimulation led to the sequence of spindle (about 10 Hz) oscillations involving both RE and TC cells. Once started, spindle oscillations lasted about 2-3 sec and were terminated as a result of depolarization of TC cells evoked by the Ca^{2+} up-regulation of I_h current (Fig. 3).

We found that the hyperpolarization of RE cells below the Cl^- reversed potential did not change the structure of spindle oscillations; however, each spindle sequence was followed

by up to several localized patterns propagating through RE network. Between spindle sequences the spike-bursts in the RE cells evoked IPSPs in TC cells which, however, were not able to trigger Ca^{2+} low-threshold spike and Na^{+} spikes. This was explained by deinactivation of the low-threshold Ca^{2+} current in TC cells which were depolarized after a spindle sequence.

In the model with finite boundary conditions, the localized waves in the RE network were terminated at the boundaries. To test longer time scales a network of RE–TC cells was stimulated with periodic boundary conditions. In the latter RE network the localized patterns continued indefinitely. This did not occur in the full RE–TC model because of the slow repolarization of TC cells. This was produced by the removal of Ca^{2+} from TC cells and led to deinactivation of the low-threshold Ca^{2+} current. When the TC membrane potential was below -64 mV, the RE-evoked IPSPs were able to trigger a low-threshold spike followed by Na^{+} spikes that led to the new sequence of spindle oscillations (see Fig. 3).

4 Discussion

Recent intracellular recordings from RE neurons at resting and hyperpolarized membrane potentials *in vivo* suggest that reversed IPSPs between RE cells can directly trigger a low-threshold spike. The model of the thalamic network examined in this paper shows that this phenomena may has an important effect on the collective dynamics of large populations of RE and TC cells. A single stimulus applied to an isolated one-dimensional RE network hyperpolarized below the Cl^{-} reversed potential triggered an isolated wave of spike-burst activity that traveled through the RE network and either terminated at the boundaries or circulated indefinitely for periodic boundary conditions (see Fig. 2). Similar localized patterns were described in the networks of cortical excitatory cells (Golomb and Amitai, 1997) and inhibitory cells (Rinzel et al., 1998); however in the latter study the wave propagation was caused by asymmetric inhibition between neurons.

In the full RE–TC network, the sequences of spindle oscillations were followed by a few localized patterns propagating inside the population of RE cells. Slow repolarization of TC cells, which were depolarized after spindle sequence, deinactivated the low-threshold Ca^{2+} current so the local RE-evoked IPSPs could trigger a new spindle sequence (see Fig. 3). The time interval between the sequences of spindle oscillations depended on the membrane potentials of the TC cells and the strengths of synaptic interconnections between the RE and TC cells.

In a previous model of spindle oscillations, new spindle sequences were triggered without persistent activity inside the RE network by including spontaneously oscillating (initiator) TC cells (Destexhe et al., 1996). In the network model studied here, the cells are almost identical and the small variability in the intrinsic properties was not strong enough to make any of these cells a pacemaker. As a result a sequence of spindle oscillations may be triggered either by the external stimulation or by localized waves traveling inside the RE network. In the one-dimensional RE–TC model considered here, periodic boundary conditions were used to keep waves traveling long enough to initiate a new spindle sequence. However we found that in a large-scale two-dimensional model of the reticular nucleus, the network may display self-sustained oscillations controlled by the maximum conductance of the low-

threshold Ca^{2+} current (in preparation). Our model predicts that the isolated reticular nucleus could initiate sequences of spindle oscillations in thalamocortical networks *in vivo*.

Acknowledgments

This research was supported by the Howard Hughes Medical Institute, the Sloan Center for Theoretical Neurobiology, Human Frontier Science Program, the Medical Research Council of Canada and the Savoy Foundation.

References

Bal T, McCormick DA (1996) What stops synchronized thalamocortical oscillations? *Neuron* 17:297-308.

Bazhenov M, Timofeev I, Steriade M and Sejnowski TJ (1998) Cellular and network models for intrathalamic augmenting responses during 10 Hz stimulation. *J. Neurophysiol.* 79:2730-2748.

Contreras D, Dossi RC, Steriade M. (1993) Electrophysiological properties of cat reticular thalamic neurones in vivo. *J. Physiol. (Lond.)* 470:273-294.

Destexhe A, Contreras D, Sejnowski TJ and Steriade M (1994a) A model of spindle rhythmicity in the isolated thalamic reticular nucleus. *J. Neurophysiol.* 72:803-818.

Destexhe A, Mainen ZF, Sejnowski T (1994b) Synthesis of models for excitable membranes, synaptic transmission and neuromodulation using a common kinetic formalism. *J. Comp. Neurosci.* 1:195-230.

Destexhe A, Bal T, McCormick DA, Sejnowski T (1996) Ionic mechanisms underlying synchronized oscillations and propagating waves in a model of ferret thalamic slices. *J. Neurophysiol.* 76:2049-2070.

Dutar P, Nicoll RA (1988) A physiological role for for GABAB receptors in the central nervous system. Nature (Lond) 332:156-158.

Enright WH, Higham DJ, Owren B, Sharp PW (1995) A survey of the explicit Runge-Kutta method. Available from ftp://ftp.cs.toronto.edu/pub/reports/na/cs-94-291.ps.Z.

Golomb D, Wang X-J, Rinzel J (1994) Synchronization properties of spindle oscillations in a thalamic reticular nucleus model. *J. Neurophysiol.* 72:1109-1126.

Golomb D, Wang X-J, Rinzel J (1996) Propagation of spindle waves in a thalamic slice model *J. Neurophysiol.* 75:750-769.

Golomb D, Amitai Y (1997) Propagating neuronal discharges in neocortical slices: Computational and experimental study. *J. Neurophysiol* 78:1199-1211.

Huguenard JR and Prince DA (1992) A novel T-type current underlies prolonged Ca^{2+}-dependent burst firing in GABAergiv neurons of rat thalamic reticular nucleus. *J. Neurosci.* 12:3804-3817.

Huguenard JR, McCormick DA (1992) Simulation of the currents involved in rhythmic oscillations in thalamic relay neurons. *J. Neurophysiol.* 68:1373-1383.

Huguenard JR, Coulter DA and McCormick DA (1991) A fast transient potassium current in thalamic relay neurons: kinetics of activation and inactivation. *J. Neurophysiol.* 66:1305-1315.

von Krosigk M, Bal T, McCormick DA (1993) Cellular mechanisms of a synchronized oscillation in the thalamus. *Science* 261:361-364.

McCormick DA and Pape HC (1990) Properties of a hyperpolarization-activated cation current and its role in rhythmic oscillation in thalamic relay neurons. *J. Physiol. Lond.* 431:291-318.

McCormick DA and Huguenard JR (1992) A model of the electrophysiological properties of thalamocortical relay neurons. *J. Neurophysiol.* 68:1384-1400.

RinzelJ, Termal D, Wang XJ, Ermentrout B (1998) Propagating activity patterns in large-scale ingibitory neuronal networks. *Science* 279:1351-1355.

Steriade M, McCormick DA, Sejnowski T (1993) Thalamocortical oscillations in the sleeping and aroused brain. *Science* 262:679-685.

Steriade M, Deschênes M, Dominich L, Mulle C (1985) Abolition of spindle oscillations in thalamic neurons disconnected from nucleus reticularis thalami. *J. Neurophysiol.* 54: 1473-1497.

Steriade M, Domich L, Oakson G, Deschênes M (1987) The deafferented reticular thalamic nucleus generates spindle rhythmicity. *J. Neurophysiol.* 57:260-273.

Steriade M, Llinás RR (1988) The functional states of the thalamus and the associated neuronal interplay. *Physiol. Rev.* 68:649-742.

Steriade M, Jones EG, Llinás RR *Thalamic oscillations and signaling* (Wiley-Interscience, New York, 1990).

Traub RD and Miles R, *Neuronal Networks of the Hippocampus*, (Cambridge: Cambridge University Press, 1991).

Ulrich D, Huguenard JR (1996) g-Aminobutyric acid type B receptor-dependent burst-firing in thalamic neurons: A dynamic clamp study. *Proc. Natl. Acad. Sci. USA* 93:13245-13249.

Ulrich D, Huguenard JR (1997) Nucleus-specific chloride homeostasis in rat thalamus. *J. Neurosci.* 17:2348-2354.